

TECHNICAL RESEARCH REPORT

A Methodology for Enumeration of Clutching Sequences Associated with Epicyclic-Type Automatic Transmission Mechanisms

by H.I. Hsieh and L.W. Tsai

T.R. 96-15



*Sponsored by
the National Science Foundation
Engineering Research Center Program,
the University of Maryland,
Harvard University,
and Industry*

A Methodology for Enumeration of Clutching Sequences Associated with Epicyclic-Type Automatic Transmission Mechanisms

Hsin-I Hsieh and Lung-Wen Tsai
University of Maryland

Reprinted from: Transmission and Driveline Systems Symposium:
Efficiency, Components, and Materials
(SP-1154)

The appearance of the ISSN code at the bottom of this page indicates SAE's consent that copies of the paper may be made for personal or internal use of specific clients. This consent is given on the condition however, that the copier pay a \$7.00 per article copy fee through the Copyright Clearance Center, Inc. Operations Center, 222 Rosewood Drive, Danvers, MA 01923 for copying beyond that permitted by Sections 107 or 108 of U.S. Copyright Law. This consent does not extend to other kinds of copying such as copying for general distribution, for advertising or promotional purposes, for creating new collective works, or for resale.

SAE routinely stocks printed papers for a period of three years following date of publication. Direct your orders to SAE Customer Sales and Satisfaction Department.

Quantity reprint rates can be obtained from the Customer Sales and Satisfaction Department.

To request permission to reprint a technical paper or permission to use copyrighted SAE publications in other works, contact the SAE Publications Group.



GLOBAL MOBILITY DATABASE

All SAE papers, standards, and selected books are abstracted and indexed in the Global Mobility Database.

No part of this publication may be reproduced in any form, in an electronic retrieval system or otherwise, without the prior written permission of the publisher.

ISSN 0148-7191

Copyright 1996 Society of Automotive Engineers, Inc.

Positions and opinions advanced in this paper are those of the author(s) and not necessarily those of SAE. The author is solely responsible for the content of the paper. A process is available by which discussions will be printed with the paper if it is published in SAE Transactions. For permission to publish this paper in full or in part, contact the SAE Publications Group.

Persons wishing to submit papers to be considered for presentation or publication through SAE should send the manuscript or a 300 word abstract of a proposed manuscript to: Secretary, Engineering Meetings Board, SAE.

Printed in USA

96-0049

A Methodology for Enumeration of Clutching Sequences Associated with Epicyclic-Type Automatic Transmission Mechanisms

Hsin-I Hsieh and Lung-Wen Tsai

University of Maryland

Copyright 1996 Society of Automotive Engineers, Inc.

ABSTRACT

This paper presents a systematic methodology for the enumeration of clutching sequences associated with epicyclic-gear-type automatic transmission mechanisms. The methodology is based on the concept that an epicyclic gear mechanism can be decomposed into several fundamental geared entities and that the overall speed ratio of an epicyclic gear mechanism can be symbolically expressed in terms of its fundamental geared entities. First, a procedure for estimating the overall speed ratio of an epicyclic gear mechanism, without specifying the exact gear dimensions, is outlined. Then, an algorithm for comparing various possible speed ratios of an epicyclic gear mechanism is described. Finally, a methodology for systematically enumerating all possible clutching sequences of an epicyclic gear mechanism is established.

1 INTRODUCTION

Most automotive automatic transmissions use epicyclic gear trains (*EGTs*) to achieve a set of speed ratios [1]. Typically, the central axis of an *EGT* is supported by bearings housed in a transmission case. This way, the *EGT* and the casing form a fractionated mechanism called the epicyclic gear mechanism (*EGM*). An *EGM* may possess two or three degrees of freedom (*DOF*) depending on whether the *EGT* is a one or two-*DOF* gear train [1]. Figure 1 shows an *EGM*, in which rotating and band clutches are denoted by C and B, respectively, and one-way clutches are replaced by band clutches for the reason of simplicity. In such a transmission mechanism, various speed ratios are obtained by clutching different links to the input power source and the casing of a transmission. A table depicting a set of speed ratios and their clutching conditions is called the *clutching sequence*. Table 1 shows the clutching sequence of the transmission shown in Fig. 1, where an X_i indicates that the corresponding clutch is activated on the i th link for that "gear." The speed ratios selected for a transmission are tailored for fuel economy and perfor-

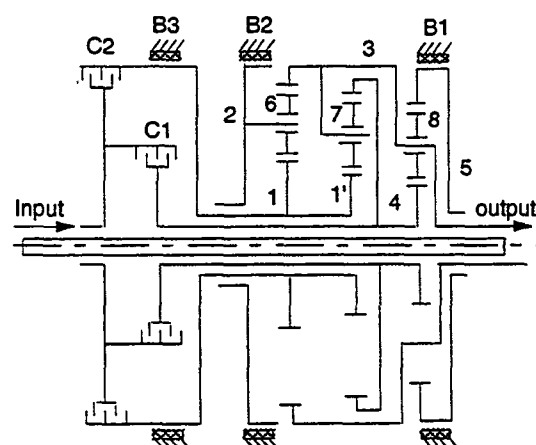


Figure 1: A Typical Transmission Mechanism

mance, a first gear for starting, a second or third gear for passing, and a high gear for fuel economy. Usually, these speed ratios are listed in a descending order, from the first gear to the last gear followed by a reverse, in a clutching sequence table.

Given such an *EGM*, we can ask ourselves the following questions. How many feasible clutching sequences can be arranged? And what is the best clutching sequence among all the feasible clutching sequences? To answer these questions, it will be necessary to develop a methodology for the enumeration of feasible clutching sequences. It will also be necessary to develop a methodology for the evaluation and comparison of various clutching sequences.

A literature survey reveals that most of the recent studies on *EGMs* have concentrated on the kinematic and static torque analyses [2-11], the power flow analysis [12-14] and the structural and dimensional synthesis [15-22]. Relative little work has been done on the enumeration of clutching sequences. Traditionally, the arrangement of a clutching sequence is accomplished by the engineer's ingenuity and intuition. This iterative approach does not necessarily result in an optimal design. Recently, Nadel and his associates [23-25] developed an artificial intelligence

Table 1: Clutching Sequence of the Mechanism Shown in Fig. 1

	Activated clutches				
Gear	C_1	C_2	B_1	B_2	B_3
First	X_4		X_5		
Second	X_4			X_2	
Third	X_4				X_1
Fourth	X_4	X_1			
Reverse		X_1	X_5		

technique for the enumeration of clutching sequences for *EGMs* made up of two simple planetary gear trains. They used a multiple abstraction level approach. The design of a transmission mechanism at the kinematic, topological and gaset levels were formulated as constraint satisfaction problems.

The artificial intelligence technique is a powerful tool for solving the transmission design problem. However, the technique involves assumptions of the design variables being discrete values in prescribed domains. Furthermore, it requires a search over all the feasible solution space. This inevitably reduces the generality and efficiency of the algorithm. In this paper, we develop a more efficient methodology to overcome this shortcoming. The methodology is based on the concept that an *EGM* can be decomposed into several fundamental geared entities (*FGEs*), the overall speed ratio of an *EGM* can be symbolically expressed in terms of the gear ratios of its *FGEs* [11], and the range of each speed ratio can be estimated before the actual dimensions of a transmission mechanism are chosen.

In what follows, we will review the definition of an *FGE* and its various modes of operation. Then, we apply these concepts for the identification and comparison of the various speed ratios of an *EGM*. Finally, we will describe a methodology for the enumeration of clutching sequences for *EGMs*.

2 OPERATION MODES OF FGEs

Canonical graph representation [26] is used to analyze the topological structure of a mechanism. The canonical graph representation of the *EGM* shown in Fig. 1 is sketched in Fig. 2(a). In a canonical graph representation, links are denoted by vertices and joints by edges. The gear pairs are represented by heavy edges, revolute joints are represented by thin edges, and the thin edges are labeled according to their axis locations in space. In addition, all the thin edged paths originated from the root have distinct edge labels. The vertices in a canonical graph can be divided into several levels as shown in Fig. 2(a). The first-level vertices represent coaxial sun gears, ring gears and carriers. The second-level vertices represent planet gears. In this study, we shall limit ourselves to those *EGMs* with their vertices distributed up to the second level.

To simplify the synthesis problem, an *EGM* is decomposed into several *FGEs* [22]. An *FGE* is a subgraph of a canonical graph formed by a single second-level vertex

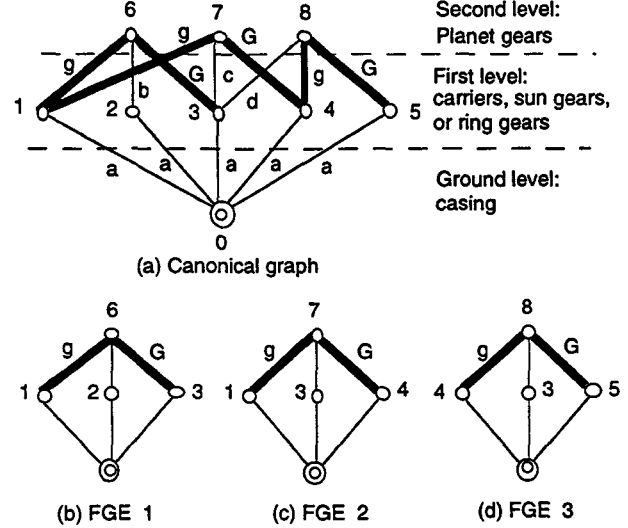


Figure 2: Canonical Graph and FGEs of the Mechanism Shown in Fig. 1

or a chain of heavy-edge connected second-level vertices together with all the lower level vertices connecting them to the root. Figures 2(b) through 2(d) show the graphs of three *FGEs* identified from Fig. 2(a). In this paper, we shall consider only those *FGEs* having a maximum of two meshing planet gears each of which is composed of a maximum of two gears. In this regard, we may be overlooking some complex *FGEs*. In our judgment, *FGEs* with more than two meshing planet gears and/or with multiple compound planet gears are not practical.

An operation mode of an *FGE* is defined as a power transmission mode which employs three first-level links as its three ports of communication to transfer power from and/or to its external environment [11]. For a set of three coaxial links, six speed ratio arrangements are possible. Let the symbol $R_{y,x}^z$ denote a speed ratio between an input link y and an output link x with reference to a fixed link z , i.e. $R_{y,x}^z = (\omega_y - \omega_z)/(\omega_x - \omega_z) = r$. Then, the other five speed ratios associated with links x, y and z can be expressed as a function of r as shown in Table 2 [11]. For example,

$$R_{y,x}^z = \frac{\omega_y - \omega_z}{\omega_x - \omega_z} = \frac{1}{\left(\frac{\omega_x - \omega_z}{\omega_y - \omega_z}\right)} = \frac{1}{R_{x,y}^z} = \frac{1}{r} \quad (1)$$

The range of a speed ratio can be classified into three kinds: (1) drive (*D*) if $R_{y,x}^z > 1$, (2) overdrive (*OD*) if $1 > R_{y,x}^z > 0$, and (3) reverse (*N*) if $0 > R_{y,x}^z$. For a given range of $R_{y,x}^z$, the ranges of the other five speed ratios can be determined as shown in Table 2.

There are four different operation modes associated with various *FGEs*. Each operation mode has several different gear train arrangements as shown in Tables 3 through 6, where one representative speed ratio is given for each gear train in terms of the three ports of communication and their gear sizes. The other five speed ratios due to kinematic inversions can be derived from Table 2. We note that most of the speed ratio ranges of these *FGEs* are known to certain extent without specifying the gear sizes. These

Table 2: Speed Ratio Relations and Their Ranges

Type of operation	$R_{y,x}^z$	$R_{x,y}^z$	$R_{y,z}^x$	$R_{z,y}^x$	$R_{x,z}^y$	$R_{z,x}^y$
Speed ratio relations	r	$\frac{1}{r}$	$1-r$	$\frac{1}{1-r}$	$\frac{r-1}{r}$	$\frac{r}{r-1}$
(a) $r > 1$	D	OD	N	N	OD	D
(b) $1 > r > 0$	OD	D	OD	D	N	N
(c) $0 > r$	N	N	D	OD	D	OD

Table 3: Operation Mode 1 - One Carrier and Two Coaxial Gears Meshing with One Planet

	(a)	(b)	(c)
Graph			
Gear train			
Speed ratio	$R_{r,s}^c = \frac{-T_s}{T_r} < 0$	$R_{r2,r1}^c = \frac{T_{r1}}{T_{r2}} \frac{T_{p'}}{T_p} > 0$	$R_{s2,s1}^c = \frac{T_{s1}}{T_{s2}} \frac{T_{p'}}{T_p} > 0$

tables provide a basis for the speed ratio analysis of a multi-stage transmission gear train.

3 OVERALL SPEED RATIO ANALYSIS

An EGM contains several coaxial links. Except for the direct drive, typically one coaxial link (called the input link) is clutched to the power source; another coaxial link (called the fixed link) is clutched to the casing, while a third coaxial link (called the output link) is permanently attached to the final reduction unit and then the differential to transmit power from an engine to the wheels. An EGM can, therefore, provide several speed ratios depending on the assignment of the input, output, and fixed links. These various speed ratios need to be estimated and arranged in a sequential order in order to arrive at a proper clutching sequence.

A methodology for expressing the overall speed ratio of an EGM in terms of its FGEs was recently developed by Hsieh and Tsai [11]. In their approach, an EGM is

Table 4: Operation Mode 2 - Three Coaxial Gears Meshing with One Planet

	(a)	(b)
Graph		
Gear train		
Speed ratio	$R_{s1,s2}^r = \frac{1 + \frac{T_r}{T_{s2}} \frac{T_{p'}}{T_p}}{1 + \frac{T_r}{T_{s1}}} > 0$	$R_{r1,r2}^s = \frac{1 + \frac{T_s}{T_{r1}} \frac{T_{p'}}{T_p}}{1 + \frac{T_s}{T_{r2}}} > 0$

decomposed into two subsystems and each subsystem is subsequently decomposed into two subsystems until the lowest level subsystem contains only one FGE. This way, the speed ratio of an EGM can be symbolically expressed in terms of the various operation modes of the FGEs shown in Tables 3 through 6. Hence, by performing the speed ratio analysis, the ranges of some speed ratios can be estimated without knowing the exact dimensions of the mechanism.

For example, when the mechanism shown in Fig. 1 is in the second gear shown in Table 1, links 2, 3, and 4 are connected to the casing, output shaft, and input shaft, respectively. Using Hsieh and Tsai's methodology [11], the overall speed ratio $R_{4,3}^2$ can be expressed as

$$\begin{aligned}
 R_{4,3}^2 &= \frac{\omega_4 - \omega_2}{\omega_3 - \omega_2} \\
 &= 1 - \frac{\omega_4 - \omega_3}{\omega_1 - \omega_3} \times \frac{\omega_1 - \omega_3}{\omega_2 - \omega_3} \\
 &= 1 - R_{4,1}^3 \times R_{1,2}^3 \quad (2)
 \end{aligned}$$

In Eq. (2), both speed ratios $R_{1,2}^3$ of FGE 1 and $R_{4,1}^3$ of FGE 2 belong to the operation mode shown in Table 3(a). From Tables 2 and 3, we obtain $R_{4,1}^3 < 0$ and $0 < R_{1,2}^3 < 1$. Hence, it can be shown that

$$R_{4,3}^2 = 1 - R_{4,1}^3 \times R_{1,2}^3 > 1 \quad (3)$$

Equation (3) implies that the range of $R_{4,3}^2$ can be estimated without specifying the gear sizes. However, it should be noted that some of the speed ratio ranges can not be estimated this way due to the fact that the dimensions of the gears are not known at this time. The following section presents an algorithm for estimating the ranges of such uncertain speed ratios.

Table 5: Operation Mode 3 - One Carrier and Two Coaxial Gears Meshing with Two Planets

	(a)	(b)	(c)
Graph			
Gear train			
Speed ratio	$1 > (R_{r,s}^c = \frac{T_s}{T_r}) > 0$	$R_{r2,r1}^c = -\frac{T_{r1}}{T_{r2}} < 0$	$R_{s2,s1}^c = -\frac{T_{s1}}{T_{s2}} < 0$

4 SPEED RATIO RELATIONS

In arranging a clutching sequence, it is desirable to achieve a single shift transition, i.e. only one clutch is turned on while another is simultaneously turned off between two successive speed ratios. Four types of single-shift transitions are possible: (a) band-to-band shift, (b) band-to-clutch shift, (c) clutch-to-clutch shift, and (d) clutch-to-band shift. In common practice, these shifts are for the following transitions. Types (a) and (c) shifts occur between two reductions or two overdrives. Type (b) shift occurs between the last reduction and the direct drive. Type (d) shift occurs between the direct drive and the first overdrive. In order to achieve single-shift transitions, two speed ratios with one commonly activated input link or fixed link are compared and arranged in a sequential order.

4.1 BAND-TO-BAND SHIFT. A band-to-band shift occurs when one band clutch is turned on while another band clutch is simultaneously turned off between two successive speed ratios. That is the fixed link is switched from one of the coaxial links to another while the input and output links remain unchanged. Hence, a band-to-band shift is feasible when there is one common input link between two speed ratios.

Let $R_{z,o}^x$ and $R_{z,o}^y$ denote two such speed ratios. Dividing $1 - R_{z,o}^x$ by $1 - R_{z,o}^y$ and after simplification, we obtain

$$\frac{1 - R_{z,o}^x}{1 - R_{z,o}^y} = 1 - R_{y,o}^x \quad (4)$$

Hence, if the ranges of $R_{y,o}^x$ and $R_{z,o}^y$ are known, the speed ratio relation between $R_{z,o}^x$ and $R_{y,o}^x$ can be derived from Eq. (4). For example, if $1 > R_{y,o}^x > 0$ and $R_{z,o}^y > 1$, then Eq. (4) yields $R_{y,o}^x > R_{z,o}^x > 1$. Similarly, if $1 >$

Table 6: Operation Mode 4 - Three Coaxial Gears Meshing with Two Planets

	(a)	(b)	(c)	(d)
Graph				
Gear train				
Speed ratio	$R_{s1,s2}^r = \frac{1 - \frac{T_r}{T_{s1}} \frac{T_{p1'}}{T_{p1}}}{1 - \frac{T_r}{T_{s2}}}$	$R_{r1,r2}^s = \frac{1 - \frac{T_s}{T_{r1}} \frac{T_{p1'}}{T_{p1}}}{1 - \frac{T_s}{T_{r2}}}$	$R_{s2,r}^{s1} = \frac{1 + \frac{T_{s1}}{T_{s2}}}{1 + \frac{T_{s1}}{T_r}} > 1$	$R_{s,r2}^{r1} = \frac{1 + \frac{T_{r1}}{T_s}}{1 + \frac{T_{r1}}{T_{r2}}} > 1$

$R_{y,o}^x > 0$ and $R_{z,o}^y < 1$, then Eq. (4) yields $1 > R_{z,o}^x > R_{y,o}^x$. Since both $R_{y,o}^x$ and $R_{z,o}^y$ can assume three possible ratio ranges, D , OD and N , nine speed ratio relations can be derived from Eq. (4) as shown in Table 7.

4.2 CLUTCH-TO-CLUTCH SHIFT. A clutch-to-clutch shift occurs when one rotating clutch is turned on while another rotating clutch is simultaneously turned off between two successive speed ratios. That is the input link is switched from one of the coaxial links to another while the fixed and output links remain unchanged. Hence, a clutch-to-clutch shift is feasible when there is one common fixed link between two speed ratios.

Let $R_{z,o}^x$ and $R_{y,o}^z$ denote two such speed ratios. Dividing $1 - R_{z,o}^x$ by $1 - R_{y,o}^z$ and after simplification, we obtain

$$\frac{1 - R_{z,o}^x}{1 - R_{y,o}^z} = 1 - R_{x,o}^y \quad (5)$$

Hence, if the ranges of $R_{y,o}^z$ and $R_{z,o}^x$ are known, the speed ratio relation between $R_{z,o}^x$ and $R_{y,o}^z$ can be derived from Eq. (5). Again, nine speed ratio relations can be derived from Eq. (5) as shown in Table 8.

5 ARRANGEMENT OF CLUTCHING SEQUENCES

We now describe a step-by-step procedure for arranging feasible clutching sequences of an EGM.

STEP 1. An EGM is decomposed into several FGEs [22]. Then, the operation modes and their ratio ranges are identified from Tables 3 through 6.

STEP 2. All possible speed ratios of an EGM are expressed in terms of its FGEs using the method developed by Hsieh and Tsai [11]. Then, Table 2 is applied to identify the ranges of some of the speed ratios. We note that some speed ratios cannot be identified in this step due to the fact that gear sizes are not specified.

STEP 3. In this step, two speed ratios sharing one

Table 9: Twelve Possible Speed Ratios Derived From the Mechanism Shown in Fig. 1

Range	Overall speed ratio
D	$R_{1,3}^4, R_{4,3}^1, R_{4,3}^5, R_{5,3}^4$
OD	$R_{2,3}^1, R_{5,3}^5$
P	$R_{2,3}^4$
N	$R_{1,3}^5, R_{1,3}^2$
Unknown	$R_{4,3}^2, R_{2,3}^5, R_{5,3}^2$

mechanism.

STEP 7. Finally, we add a reverse drive to the clutching sequence. In order to reduce the number of rotating and band clutches, we apply two of the clutches designed for the forward drives for the reverse drive.

6 EXAMPLE

The mechanism shown in Fig. 1 is composed of a Simpson gear train and a simple planetary gear train. Assuming that the sizes of the sun gears are in the descending order of gear 1 > gear 1' > gear 4, and the sizes of the ring gears are in the descending order of gear 3 > gear 4 > gear 5. The procedure for deriving possible clutching sequences is as follows:

STEP 1. The three *FGEs* are shown in Fig. 2. Since all three *FGEs* belong to the operation mode shown in Table 3(a), we have $R_{3,1}^2 < 0$, $R_{4,1'}^3 < 0$, and $R_{5,4}^3 < 0$. All the other speed ratios of the *FGEs* due to kinematic inversion can be found from Table 2.

STEP 2. Since there are five coaxial links and link 3 has already been assigned as the output link, a total of twelve clutching conditions and, therefore, twelve overall speed ratios are possible. Each of these speed ratios can be expressed in terms of the above three *FGEs* using the methodology developed by Hsieh and Tsai [11]. After some algebra, we obtain twelve speed ratios grouped according to their ratio ranges as shown in Table 9.

STEP 3. Selecting three out of the four coaxial links at one time, yields four sets of three coaxial links which can be divided into three groups. The first group includes one set of three coaxial links (1, 4, 5), the second group includes two sets of three coaxial links (1, 2, 4) and (1, 2, 5), and the third group includes one set of three coaxial links (2, 4, 5).

For the coaxial links (1, 4, 5), we use the fact that $R_{4,3}^1 > 1$ and $R_{5,3}^4 > 1$ from Table 9 to begin our evaluation. By assigning $x = 1$, $y = 4$, and $z = 5$ in Table 7, we obtain $R_{5,3}^4 > 1 > R_{1,3}^5$. Assigning $x = 5$, $y = 4$, and $z = 1$ in Table 7, we obtain $R_{1,3}^4 > 1 > R_{5,3}^2$. And assigning $x = 5$, $y = 1$, and $z = 4$ in Table 7, we obtain $R_{4,3}^2 > R_{1,3}^5 > 1$.

For the coaxial links (1, 2, 5), we obtain $R_{1,3}^2 < 0$ and $1 > R_{5,3}^5 > 0$ from Table 9. By assigning $x = 2$, $y = 1$, and $z = 5$ in Table 7, we obtain $1 > R_{1,3}^5 > R_{5,3}^2$. By assigning $x = 5$, $y = 1$, and $z = 2$ in Table 7, we obtain $1 > R_{2,3}^1 > R_{5,3}^5$. Note that from the above two operations the range of $R_{5,3}^2$ is identified as $R_{5,3}^2 < 1$. Two possible subcases exist: (1) $1 > R_{2,3}^1 > 0$ and (2) $0 > R_{2,3}^1$. We let $x = 5$, $y = 2$, $z = 1$ in Table 7 and evaluate each subcase

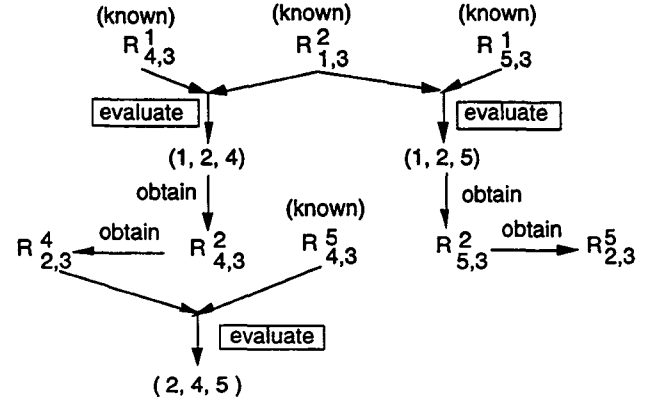


Figure 3: Speed Ratio Evaluation For the Mechanism Shown in Fig. 1

separately. If $1 > R_{2,3}^1 > 0$, then $0 > R_{5,3}^5 > R_{1,3}^2$; and if $0 > R_{2,3}^1$, then $0 > R_{1,3}^2 > R_{5,3}^5$. After this step, the ranges of $R_{2,3}^1$ and $R_{5,3}^5$ become known.

Similarly, the ranges of $R_{2,3}^4$ and $R_{4,3}^2$ are obtained by performing the second-group evaluation for the coaxial links (1, 2, 4).

For each subcase, we obtain the ranges of $R_{2,3}^4$, $R_{4,3}^2$, $R_{5,3}^5$, and $R_{5,3}^2$ which enable us to perform the first-group evaluation for the set of three coaxial links (2, 4, 5). The sequence of evaluation are schematically depicted in Fig. 3.

STEP 4. In this step, we compare two speed ratios with a common fixed link. The procedure is similar to that of Step 3. For example, the two speed ratios $R_{4,3}^1$ and $R_{2,3}^4$ can be compared by applying Table 8 to the set of three coaxial links (1, 2, 4).

STEP 5. After completing the speed ratio evaluations, we obtain two families of speed ratio ranges. In each family, there are six drives (D), three overdrives (OD), and three reverses (N) as shown in Tables 10 and 11. We note that there are two sets of three reductions in each family.

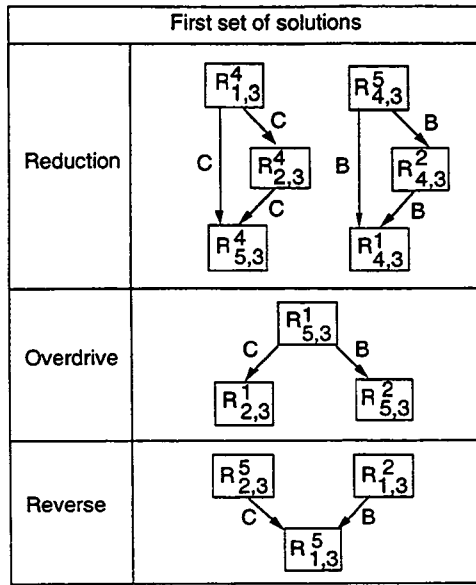
STEP 6. In this step, we add a direct-drive between the last reduction and the overdrive. For example, the input clutches C_1 and C_2 shown in Table 1 are applied for the direct drive based on Rule 3. Hence, with one overdrive, we obtain four feasible four-speed clutching sequences as shown in Table 12. If two overdrives are permitted, eight five-speed clutching sequences are feasible.

STEP 7. Finally, a reverse drive is added to each clutching sequence. Table 1 shows one feasible clutching sequence with rotating clutches attached to links 1 and 4, and band clutches attached to links 1, 2, and 5. This clutching sequence has been applied in several four-speed transmissions.

7 RESULTS

A computer program for the enumeration of clutching sequences has been written in MATHEMATICA language [27]. The algorithm obviates the necessity of inputting the exact gear dimensions of an *EGM*. The designer only needs to specify the vertex-to-vertex adjacent matrix of an *EGM*, the number and type of gears on each link, and the information containing the approximate gear sizes ar-

Table 10: Speed Ratio Flow Chart Derived From the Mechanism Shown in Fig. 1 - Family 1



ranged in a descending order. The program starts with the identification of the various operation modes of an *EGM* and arriving at all feasible clutching sequences. We have tested the program on various gear trains. As a result, we obtain two three-speed and two four-speed clutching sequences for each of the Simpson, Ravigneaux, and Type-6206 gear sets [1] as shown in Figs. 4, 5, and 6.

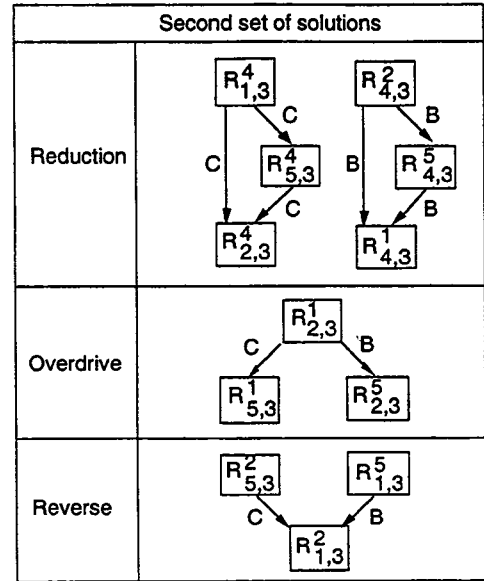
The clutching sequence shown in Figs. 4(b) and 5(b) have been used in most three-speed automatic transmissions (See [1] for examples). The clutching sequence shown in Fig. 6(b) has been applied in the HYDRA-MATIC 3L80 transmission. The clutching sequence shown in Fig. 6(d) has been used in HYDRA-MATIC 4T60 and Ford Axod. The other clutching sequences shown appear to be new.

8 CONCLUSION

In this study, we have concentrated on three issues related to the enumeration of clutching sequences associated with epicyclic gear mechanisms from the kinematic point of view.

First, a procedure for estimating the overall speed ratio of an *EGM*, without specifying the exact gear dimensions, is outlined. Then, an algorithm for comparing various possible speed ratios of an *EGM* is described. Finally, a methodology for systematically enumerating all possible clutching sequences of an *EGM* is established. The methodology has been demonstrated by a transmission gear set making up of three simple planetary gear trains. In addition, a computer program has been written in MATHEMATICA [27] and successfully tested on various transmission gear trains including the Simpson, Ravigneaux, and Type-6206 gear sets. It is shown that all possible clutching sequences of an *EGM* can be systematically enumerated. It is hoped that this methodology will provide transmission designers an efficient tool for enumer-

Table 11: Speed Ratio Flow Chart Derived From the Mechanism Shown in Fig. 1 - Family 2



ating feasible clutching sequences of an *EGM*.

In this paper, the physical layout of a transmission mechanism has not been studied. It is possible that some of the clutching sequences enumerated may lead to infeasible mechanical layout. This is a subject of future study.

9 NOMENCLATURE

D	Drive, $R_{x,y}^z > 1$
EGM	Epicyclic gear mechanism
FGE	Fundamental geared entity
N	Reverse, $R_{x,y}^z < 0$
OD	Overdrive, $1 > R_{x,y}^z > 0$
P	Positive speed ratio, $R_{x,y}^z > 0$
$N_{p,x}$	Gear ratio defined by a planet gear p and a sun or a ring gear x . $N_{p,x} = \pm T_p/T_x$, where T_p and T_x denote the number of teeth on a planet gear and a sun or ring gear, respectively, and the positive or negative sign depends on whether x is a ring or sun gear.
$R_{x,y}^z$	Speed ratio between an input link x and an output link y with reference to a fixed link z , $R_{x,y}^z = (\omega_x - \omega_z)/(\omega_y - \omega_z)$.
c	Carrier
r	Ring gear
s	Sun gear
ω_i	Angular velocity of link i

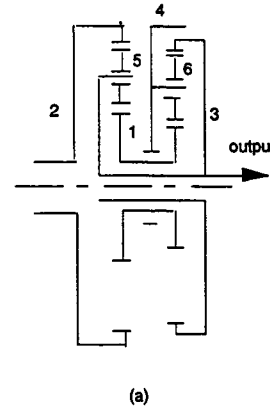
10 ACKNOWLEDGMENT

This work was supported in part by the U.S. Department of Energy under Grant No. DEF05-88 ER 13977. Such support does not constitute an endorsement by the supporting agency of the views expressed in the paper.

Table 12: Four Four-Speed Clutching Sequences Derived From the Mechanism Shown in Fig. 1

First set of solutions									
Gear	Activated clutches					Gear	Activated clutches		
	C ₁	C ₂	B ₁	B ₂	B ₃		C ₁	C ₂	C ₃
First	X ₄			X ₅		First	X ₁		X ₄
Second	X ₄			X ₂		Second		X ₂	X ₄
Third	X ₄				X ₁	Third			X ₅
Fourth	X ₄	X ₁				Fourth		X ₂	X ₅
Reverse		X ₁	X ₅			Reverse	X ₁		

Second set of solutions									
Gear	Activated clutches					Gear	Activated clutches		
	C ₁	C ₂	B ₁	B ₂	B ₃		C ₁	C ₂	C ₃
First	X ₄		X ₂			First	X ₁		X ₄
Second	X ₄			X ₅		Second		X ₅	X ₄
Third	X ₄				X ₁	Third		X ₂	X ₄
Fourth	X ₄	X ₁				Fourth		X ₅	X ₂
Reverse		X ₁		X ₅		Reverse	X ₁		



	Activated clutches			
Gear	C ₁	C ₂	B ₁	B ₂
First	X ₂		X ₄	
Second	X ₂			X ₁
Third	X ₂	X ₁		
Reverse		X ₁	X ₄	

(b)

	Activated clutches			
Gear	C ₁	C ₂	B ₁	B ₂
First	X ₁		X ₂	
Second		X ₄	X ₂	
Third	X ₁	X ₄		
Reverse	X ₁			X ₄

(c)

	Activated clutches				
Gear	C ₁	C ₂	B ₁	B ₂	B ₃
First	X ₁		X ₂		
Second		X ₄	X ₂		
Third	X ₁	X ₄			
Fourth		X ₄		X ₁	
Reverse	X ₁				X ₄

(d)

	Activated clutches				
Gear	C ₁	C ₂	C ₃	B ₁	B ₂
First	X ₂			X ₄	
Second	X ₂				X ₁
Third	X ₂	X ₄			
Fourth		X ₄			X ₁
Reverse			X ₁	X ₄	

(e)

Figure 4: Four Feasible Clutching Sequences Derived From Simpson Gear Set

11 REFERENCES

1. Tsai, L.W., Maki, E. R., Liu, T., and Kapil, N. G., "The Categorization of Planetary Gear Trains For Automatic Transmissions According to Kinematic Topology," SAE paper No. 885062, *SAE XXII FISITA '88, Automotive Systems Technology: The Future*, P-211, Vol. 1, pp. 1.513-1.521, 1988.
2. Levai, Z., "Theory of Epicyclic Gears and Epicyclic Change-Speed Gears", Doctoral Dissertation, Budapest, 1964.
3. Gackstetter, G., "Leistungsverzweigung bei der stufenlosen Drehzahlregelung mit vierwelligen Planetengetrieben," VDI-Z, Vol. 108, No.6, pp. 210-214, 1966.
4. Polder, J.W., "A Network Theory for Variable Epicyclic Gear Trains," Ph.D. Dissertation, University of Technology, Eindhoven, Netherland, 1969.
5. Freudenstein, F., and Yang, A. T., "Kinematics and Statics of Coupled Epicyclic Spur Gear Trains," *Journal of Mechanism and Machine Theory*, Vol. 7, pp. 263-375, 1972.
6. Tsai, L.W., "An Algorithm for the Kinematic Analysis of Epicyclic Gear Trains," *Proc. Sixth Applied Mechanisms Conference*, Kansas City, 1985.
7. Belfiore, N. P., and Pennestri, E., "Kinematic and Static Force Analysis of Epicyclic Gear Trains," *Proceedings 1st National Applied Mechanisms and Robotics*, Cincinnati, OH, Vol. 1, Paper No. AMR-6B-1, 1989.
8. Hedman, A., "Mechanical Transmission Systems: A General Computer Based Method of Analysis," Ph.D. Dissertation, Div. of Machine Elements, Chalmers University of Technology, Goteborg, Sweden, 1989.
9. Hedman, A., "Computer Aided Analysis of General Mechanical Transmission Systems," *Proc. Second Int'l Conf. on New Developments in Powertrain and Chassis Engineering*, Strassburg, France, pp. 193-197, 1989.
10. Hedman, A., "Transmission Analysis - Automatic Derivation of Relationships," *ASME Journal of Mechanical Design*, Vol. 115, No. 4, pp. 1031-1037, 1993.
11. Hsieh, H.I., and Tsai, L.W., "Kinematic Analysis of Epicyclic-Type Transmission Mechanisms Using the Concept of Fundamental Geared Entities," *Proc. of the ASME 1995 Design Eng. Tech. Conferences, Advances in Design Automation*, Vol. 1, pp. 545-552, Boston, Mass, 1995.
12. Saggere, L., and Olson, D. G., "A Simplified Approach for Force and Power-Flow Analysis of Compound Epicyclic Spur-Gear Trains," *Proc. ASME Advances in Design Automation*, DE-Vol. 44-2, pp. 83-89, 1992.
13. Pennestri, E., and Freudenstein, F., "A Systematic Approach to Power-Flow and Static Force Analysis in Epicyclic Spur-Gear Trains," *ASME Journal of Mechanical Design*, Vol. 115, No. 3, pp. 639-644, 1993.
14. Pennestri, E., Sinatra, R., and Belfiore, N. P., "A Catalog of Automotive Transmissions with Kinematic and Power-Flow Analysis," *Proc. National Applied Mechanisms and Robotics*, Cincinnati, OH, No. AMR-93-057, pp. 1-8, 1993.

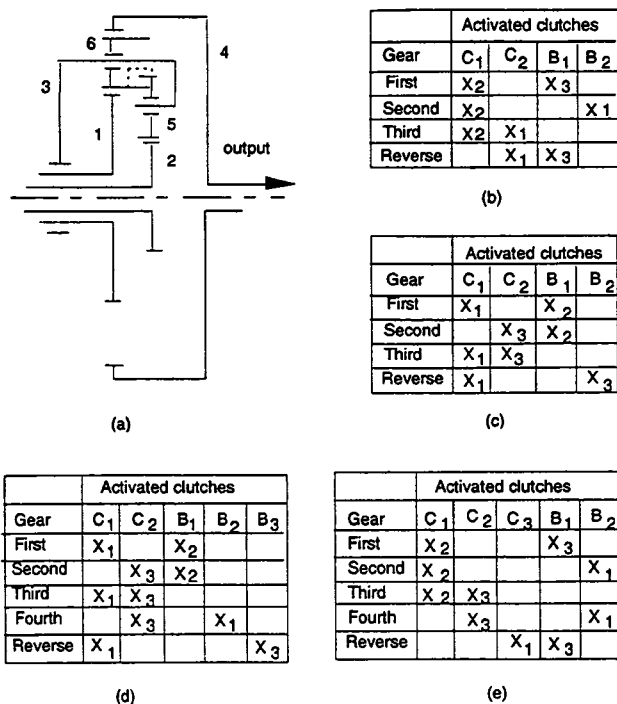


Figure 5: Four Feasible Clutching Sequences Derived From Ravigneaux Gear Set

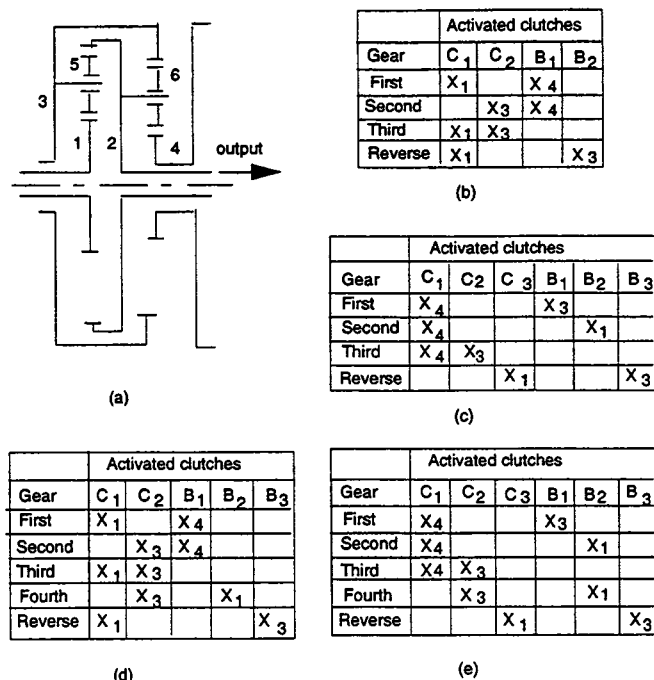


Figure 6: Four Feasible Clutching Sequences Derived From Type 6206 Gear Set

15. Buchsbaum, F., and Freudenstein, F., "Synthesis of Kinematic Structure of Geared Kinematic Chains and Other Mechanisms," *Journal of Mechanisms and Machine Theory*, Vol. 5, pp. 357-392, 1970.
16. Mruthyunjaya, T.S., and Ravisankar, R., "Computerized Synthesis of the Structure of Geared Kinematic Chains," *Journal of Mechanisms and Machine Theory*, Vol. 20, pp. 367-387, 1985.
17. Tsai, L.W., and Lin, C.C., "The Creation of Non-Fractionated Two-Degree-of-Freedom Epicyclic Gear Trains," *ASME J. of Mechanisms, Transmissions, and Automation in Design*, Vol. 111, pp. 524-529, 1989.
18. Hylander, M., "Generation and Optimization of Epicyclic Transmission Designs," VDI Berichte 1007, 1992.
19. Hylander, M., "On Synthesis in Epicyclic Transmission Design," *Machine and Vehicle Design*, Chalmers University of Technology, Goteborg, Sweden, Report No. 1993-02-26, 1993.
20. Mogalapalli, S.N., Magrab, E.B., and Tsai, L.W., "A CAD System for the Optimization of Gear Ratios for Automotive Automatic Transmissions," *SAE Int'l. Congress and Exposition*, SAE paper No. 930675, Automotive Transmissions and Drivelines, SP-965, pp. 111-118, 1993.
21. Chatterjee, G., and Tsai, L.W., "Enumeration of Epicyclic-Type Automatic Transmission Gear Trains," *SAE International Congress and Exposition*,

- Paper No. 941012, Transmission and Driveline Developments, SP- 1032, pp. 153-164, 1994.
22. Chatterjee, G., and Tsai, L.W., "Computer-Aided Sketching of Epicyclic-Type Automatic Transmission Gear Trains," *Proc. of the ASME 1994 Design Technical Conferences*, DE-Vol. 71, Machine Elements and Machine Dynamics, pp. 275-282, 1994.
23. Nadel, B.A., and Lin, J., "Automobile Transmission Design as a Constraint Satisfaction Problem: First Results," *Proc. 7th IEEE Conf. on Artificial Intelligence Applications*, pp. 248-256, 1991.
24. Nadel, B.A., and Lin, J., "Automobile Transmission Design as a Constraint Satisfaction Problem: Modeling the Kinematic Level," *Artificial Intelligence for Engineering Design, Analysis and Manufacturing*, Vol. 5, No. 3, pp. 137-171, 1991.
25. Nadel, B.A., Wu, X., and Kagan, D., "Multiple Abstraction Levels in Automobile Transmission Design: Constraint Satisfaction Formulation and Implementation," *Int'l. Journal of Expert Systems*, Vol. 6, No. 4, pp. 489- 559, 1993.
26. Tsai, L.W., "The Kinematics of Spatial Robotic Bevel-Gear Trains," *IEEE Journal of Robotics and Automation*, Vol. 4, No. 2, pp. 150-155, 1988.
27. Wolfram, S., "Mathematica: A System For Doing Mathematics By Computer," Addison-Wesley, New York, NY, 1991.

A Methodology for Enumeration of Clutching Sequences Associated with Epicyclic-Type Automatic Transmission Mechanisms

Hsin-I Hsieh and Lung-Wen Tsai
University of Maryland

Reprinted from: **Transmission and Driveline Systems Symposium:
Efficiency, Components, and Materials
(SP-1154)**

The appearance of the ISSN code at the bottom of this page indicates SAE's consent that copies of the paper may be made for personal or internal use of specific clients. This consent is given on the condition however, that the copier pay a \$7.00 per article copy fee through the Copyright Clearance Center, Inc. Operations Center, 222 Rosewood Drive, Danvers, MA 01923 for copying beyond that permitted by Sections 107 or 108 of U.S. Copyright Law. This consent does not extend to other kinds of copying such as copying for general distribution, for advertising or promotional purposes, for creating new collective works, or for resale.

SAE routinely stocks printed papers for a period of three years following date of publication. Direct your orders to SAE Customer Sales and Satisfaction Department.

Quantity reprint rates can be obtained from the Customer Sales and Satisfaction Department.

To request permission to reprint a technical paper or permission to use copyrighted SAE publications in other works, contact the SAE Publications Group.



GLOBAL MOBILITY DATABASE

All SAE papers, standards, and selected books are abstracted and indexed in the Global Mobility Database.

No part of this publication may be reproduced in any form, in an electronic retrieval system or otherwise, without the prior written permission of the publisher.

ISSN 0148-7191

Copyright 1996 Society of Automotive Engineers, Inc.

Positions and opinions advanced in this paper are those of the author(s) and not necessarily those of SAE. The author is solely responsible for the content of the paper. A process is available by which discussions will be printed with the paper if it is published in SAE Transactions. For permission to publish this paper in full or in part, contact the SAE Publications Group.

Persons wishing to submit papers to be considered for presentation or publication through SAE should send the manuscript or a 300 word abstract of a proposed manuscript to: Secretary, Engineering Meetings Board, SAE.

Printed in USA

96-0049

A Methodology for Enumeration of Clutching Sequences Associated with Epicyclic-Type Automatic Transmission Mechanisms

Hsin-I Hsieh and Lung-Wen Tsai
University of Maryland

Copyright 1996 Society of Automotive Engineers, Inc.

ABSTRACT

This paper presents a systematic methodology for the enumeration of clutching sequences associated with epicyclic-gear-type automatic transmission mechanisms. The methodology is based on the concept that an epicyclic gear mechanism can be decomposed into several fundamental geared entities and that the overall speed ratio of an epicyclic gear mechanism can be symbolically expressed in terms of its fundamental geared entities. First, a procedure for estimating the overall speed ratio of an epicyclic gear mechanism, without specifying the exact gear dimensions, is outlined. Then, an algorithm for comparing various possible speed ratios of an epicyclic gear mechanism is described. Finally, a methodology for systematically enumerating all possible clutching sequences of an epicyclic gear mechanism is established.

1 INTRODUCTION

Most automotive automatic transmissions use epicyclic gear trains (*EGTs*) to achieve a set of speed ratios [1]. Typically, the central axis of an *EGT* is supported by bearings housed in a transmission case. This way, the *EGT* and the casing form a fractionated mechanism called the epicyclic gear mechanism (*EGM*). An *EGM* may possess two or three degrees of freedom (*DOF*) depending on whether the *EGT* is a one or two-*DOF* gear train [1]. Figure 1 shows an *EGM*, in which rotating and band clutches are denoted by *C* and *B*, respectively, and one-way clutches are replaced by band clutches for the reason of simplicity. In such a transmission mechanism, various speed ratios are obtained by clutching different links to the input power source and the casing of a transmission. A table depicting a set of speed ratios and their clutching conditions is called the *clutching sequence*. Table 1 shows the clutching sequence of the transmission shown in Fig. 1, where an X_i indicates that the corresponding clutch is activated on the i th link for that "gear." The speed ratios selected for a transmission are tailored for fuel economy and perfor-

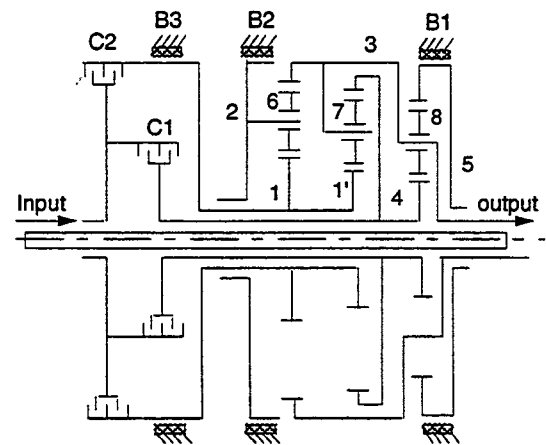


Figure 1: A Typical Transmission Mechanism

mance, a first gear for starting, a second or third gear for passing, and a high gear for fuel economy. Usually, these speed ratios are listed in a descending order, from the first gear to the last gear followed by a reverse, in a clutching sequence table.

Given such an *EGM*, we can ask ourselves the following questions. How many feasible clutching sequences can be arranged? And what is the best clutching sequence among all the feasible clutching sequences? To answer these questions, it will be necessary to develop a methodology for the enumeration of feasible clutching sequences. It will also be necessary to develop a methodology for the evaluation and comparison of various clutching sequences.

A literature survey reveals that most of the recent studies on *EGMs* have concentrated on the kinematic and static torque analyses [2-11], the power flow analysis [12-14] and the structural and dimensional synthesis [15-22]. Relative little work has been done on the enumeration of clutching sequences. Traditionally, the arrangement of a clutching sequence is accomplished by the engineer's ingenuity and intuition. This iterative approach does not necessarily result in an optimal design. Recently, Nadel and his associates [23-25] developed an artificial intelligence

Table 1: Clutching Sequence of the Mechanism Shown in Fig. 1

	Activated clutches				
Gear	C_1	C_2	B_1	B_2	B_3
First	X_4		X_5		
Second	X_4			X_2	
Third	X_4				X_1
Fourth	X_4	X_1			
Reverse		X_1	X_5		

technique for the enumeration of clutching sequences for *EGMs* made up of two simple planetary gear trains. They used a multiple abstraction level approach. The design of a transmission mechanism at the kinematic, topological and gearset levels were formulated as constraint satisfaction problems.

The artificial intelligence technique is a powerful tool for solving the transmission design problem. However, the technique involves assumptions of the design variables being discrete values in prescribed domains. Furthermore, it requires a search over all the feasible solution space. This inevitably reduces the generality and efficiency of the algorithm. In this paper, we develop a more efficient methodology to overcome this shortcoming. The methodology is based on the concept that an *EGM* can be decomposed into several fundamental geared entities (*FGEs*), the overall speed ratio of an *EGM* can be symbolically expressed in terms of the gear ratios of its *FGEs* [11], and the range of each speed ratio can be estimated before the actual dimensions of a transmission mechanism are chosen.

In what follows, we will review the definition of an *FGE* and its various modes of operation. Then, we apply these concepts for the identification and comparison of the various speed ratios of an *EGM*. Finally, we will describe a methodology for the enumeration of clutching sequences for *EGMs*.

2 OPERATION MODES OF FGES

Canonical graph representation [26] is used to analyze the topological structure of a mechanism. The canonical graph representation of the *EGM* shown in Fig. 1 is sketched in Fig. 2(a). In a canonical graph representation, links are denoted by vertices and joints by edges. The gear pairs are represented by heavy edges, revolute joints are represented by thin edges, and the thin edges are labeled according to their axis locations in space. In addition, all the thin edged paths originated from the root have distinct edge labels. The vertices in a canonical graph can be divided into several levels as shown in Fig. 2(a). The first-level vertices represent coaxial sun gears, ring gears and carriers. The second-level vertices represent planet gears. In this study, we shall limit ourselves to those *EGMs* with their vertices distributed up to the second level.

To simplify the synthesis problem, an *EGM* is decomposed into several *FGEs* [22]. An *FGE* is a subgraph of a canonical graph formed by a single second-level vertex

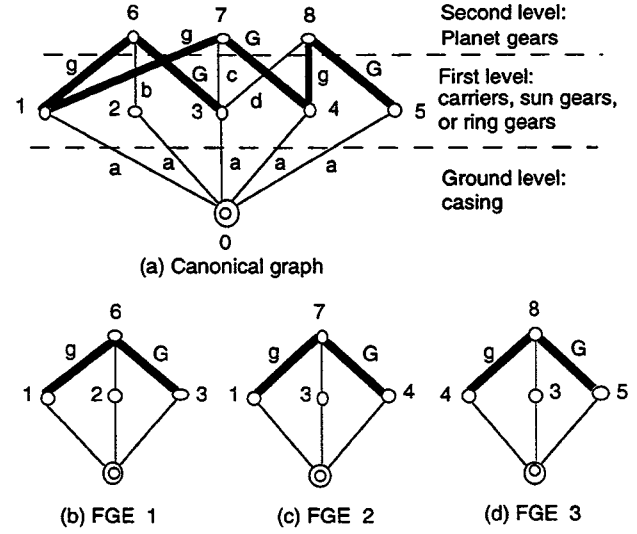


Figure 2: Canonical Graph and FGEs of the Mechanism Shown in Fig. 1

or a chain of heavy-edge connected second-level vertices together with all the lower level vertices connecting them to the root. Figures 2(b) through 2(d) show the graphs of three *FGEs* identified from Fig. 2(a). In this paper, we shall consider only those *FGEs* having a maximum of two meshing planet gears each of which is composed of a maximum of two gears. In this regard, we may be overlooking some complex *FGEs*. In our judgment, *FGEs* with more than two meshing planet gears and/or with multiple compound planet gears are not practical.

An operation mode of an *FGE* is defined as a power transmission mode which employs three first-level links as its three ports of communication to transfer power from and/or to its external environment [11]. For a set of three coaxial links, six speed ratio arrangements are possible. Let the symbol $R_{y,x}^z$ denote a speed ratio between an input link y and an output link x with reference to a fixed link z , i.e. $R_{y,x}^z = (\omega_y - \omega_z)/(\omega_x - \omega_z) = r$. Then, the other five speed ratios associated with links x, y and z can be expressed as a function of r as shown in Table 2 [11]. For example,

$$R_{y,x}^z = \frac{\omega_y - \omega_z}{\omega_x - \omega_z} = \frac{1}{\left(\frac{\omega_x - \omega_z}{\omega_y - \omega_z}\right)} = \frac{1}{R_{x,y}^z} = \frac{1}{r} \quad (1)$$

The range of a speed ratio can be classified into three kinds: (1) drive (*D*) if $R_{y,x}^z > 1$, (2) overdrive (*OD*) if $1 > R_{y,x}^z > 0$, and (3) reverse (*N*) if $0 > R_{y,x}^z$. For a given range of $R_{y,x}^z$, the ranges of the other five speed ratios can be determined as shown in Table 2.

There are four different operation modes associated with various *FGEs*. Each operation mode has several different gear train arrangements as shown in Tables 3 through 6, where one representative speed ratio is given for each gear train in terms of the three ports of communication and their gear sizes. The other five speed ratios due to kinematic inversions can be derived from Table 2. We note that most of the speed ratio ranges of these *FGEs* are known to certain extent without specifying the gear sizes. These

Table 2: Speed Ratio Relations and Their Ranges

Type of operation	$R_{y,x}^z$	$R_{x,y}^z$	$R_{y,z}^x$	$R_{z,y}^x$	$R_{x,z}^y$	$R_{z,x}^y$
Speed ratio relations	r	$\frac{1}{r}$	$1-r$	$\frac{1}{1-r}$	$\frac{r-1}{r}$	$\frac{r}{r-1}$
(a) $r > 1$	D	OD	N	N	OD	D
(b) $1 > r > 0$	OD	D	OD	D	N	N
(c) $0 > r$	N	N	D	OD	D	OD

Table 3: Operation Mode 1 - One Carrier and Two Coaxial Gears Meshing with One Planet

	(a)	(b)	(c)
Graph			
Gear train			
Speed ratio	$R_{r,s}^c = \frac{-T_s}{T_r} < 0$	$R_{r2,r1}^c = \frac{T_{r1}}{T_{r2}} \frac{T_{p'}}{T_p} > 0$	$R_{s2,s1}^c = \frac{T_{s1}}{T_{s2}} \frac{T_{p'}}{T_p} > 0$

tables provide a basis for the speed ratio analysis of a multi-stage transmission gear train.

3 OVERALL SPEED RATIO ANALYSIS

An EGM contains several coaxial links. Except for the direct drive, typically one coaxial link (called the input link) is clutched to the power source; another coaxial link (called the fixed link) is clutched to the casing, while a third coaxial link (called the output link) is permanently attached to the final reduction unit and then the differential to transmit power from an engine to the wheels. An EGM can, therefore, provide several speed ratios depending on the assignment of the input, output, and fixed links. These various speed ratios need to be estimated and arranged in a sequential order in order to arrive at a proper clutching sequence.

A methodology for expressing the overall speed ratio of an EGM in terms of its FGEs was recently developed by Hsieh and Tsai [11]. In their approach, an EGM is

Table 4: Operation Mode 2 - Three Coaxial Gears Meshing with One Planet

	(a)	(b)
Graph		
Gear train		
Speed ratio	$R_{s1,s2}^r = \frac{1 + \frac{T_r}{T_{s2}} \frac{T_{p'}}{T_p}}{1 + \frac{T_r}{T_{s1}}} > 0$	$R_{r1,r2}^s = \frac{1 + \frac{T_s}{T_{r1}} \frac{T_{p'}}{T_p}}{1 + \frac{T_s}{T_{r2}}} > 0$

decomposed into two subsystems and each subsystem is subsequently decomposed into two subsystems until the lowest level subsystem contains only one FGE. This way, the speed ratio of an EGM can be symbolically expressed in terms of the various operation modes of the FGEs shown in Tables 3 through 6. Hence, by performing the speed ratio analysis, the ranges of some speed ratios can be estimated without knowing the exact dimensions of the mechanism.

For example, when the mechanism shown in Fig. 1 is in the second gear shown in Table 1, links 2, 3, and 4 are connected to the casing, output shaft, and input shaft, respectively. Using Hsieh and Tsai's methodology [11], the overall speed ratio $R_{4,3}^2$ can be expressed as

$$\begin{aligned}
 R_{4,3}^2 &= \frac{\omega_4 - \omega_2}{\omega_3 - \omega_2} \\
 &= 1 - \frac{\omega_4 - \omega_3}{\omega_1 - \omega_3} \times \frac{\omega_1 - \omega_3}{\omega_2 - \omega_3} \\
 &= 1 - R_{4,1}^3 \times R_{1,2}^3
 \end{aligned} \quad (2)$$

In Eq. (2), both speed ratios $R_{1,2}^3$ of FGE 1 and $R_{4,1}^3$ of FGE 2 belong to the operation mode shown in Table 3(a). From Tables 2 and 3, we obtain $R_{4,1}^3 < 0$ and $0 < R_{1,2}^3 < 1$. Hence, it can be shown that

$$R_{4,3}^2 = 1 - R_{4,1}^3 \times R_{1,2}^3 > 1 \quad (3)$$

Equation (3) implies that the range of $R_{4,3}^2$ can be estimated without specifying the gear sizes. However, it should be noted that some of the speed ratio ranges can not be estimated this way due to the fact that the dimensions of the gears are not known at this time. The following section presents an algorithm for estimating the ranges of such uncertain speed ratios.

Table 5: Operation Mode 3 - One Carrier and Two Coaxial Gears Meshing with Two Planets

	(a)	(b)	(c)
Graph			
Gear train			
Speed ratio	$1 > (R_{r,s}^c = \frac{T_s}{T_r}) > 0$	$R_{r2,r1}^c = \frac{-T_{r1}}{T_{r2}} < 0$	$R_{s2,s1}^c = \frac{-T_{s1}}{T_{s2}} < 0$

4 SPEED RATIO RELATIONS

In arranging a clutching sequence, it is desirable to achieve a single shift transition, i.e. only one clutch is turned on while another is simultaneously turned off between two successive speed ratios. Four types of single-shift transitions are possible: (a) band-to-band shift, (b) band-to-clutch shift, (c) clutch-to-clutch shift, and (d) clutch-to-band shift. In common practice, these shifts are for the following transitions. Types (a) and (c) shifts occur between two reductions or two overdrives. Type (b) shift occurs between the last reduction and the direct drive. Type (d) shift occurs between the direct drive and the first overdrive. In order to achieve single-shift transitions, two speed ratios with one commonly activated input link or fixed link are compared and arranged in a sequential order.

4.1 BAND-TO-BAND SHIFT. A band-to-band shift occurs when one band clutch is turned on while another band clutch is simultaneously turned off between two successive speed ratios. That is the fixed link is switched from one of the coaxial links to another while the input and output links remain unchanged. Hence, a band-to-band shift is feasible when there is one common input link between two speed ratios.

Let $R_{z,o}^x$ and $R_{z,o}^y$ denote two such speed ratios. Dividing $1 - R_{z,o}^x$ by $1 - R_{z,o}^y$ and after simplification, we obtain

$$\frac{1 - R_{z,o}^x}{1 - R_{z,o}^y} = 1 - R_{y,o}^x \quad (4)$$

Hence, if the ranges of $R_{y,o}^x$ and $R_{z,o}^y$ are known, the speed ratio relation between $R_{z,o}^x$ and $R_{z,o}^y$ can be derived from Eq. (4). For example, if $1 > R_{y,o}^x > 0$ and $R_{z,o}^y > 1$, then Eq. (4) yields $R_{z,o}^x > R_{z,o}^y > 1$. Similarly, if $1 >$

Table 6: Operation Mode 4 - Three Coaxial Gears Meshing with Two Planets

	(a)	(b)	(c)	(d)
Graph				
Gear train				
Speed ratio	$R_{s1,s2}^r = \frac{1 - \frac{T_r}{T_{s1}} \frac{T_{p1'}}{T_{p1}}}{1 - \frac{T_r}{T_{s2}}}$	$R_{r1,r2}^s = \frac{1 - \frac{T_s}{T_{r1}} \frac{T_{p1'}}{T_{p1}}}{1 - \frac{T_s}{T_{r2}}}$	$R_{s2,r}^{s1} = \frac{1 + \frac{T_{s1}}{T_{s2}}}{1 + \frac{T_{s1}}{T_r}} > 1$	$R_{s,r2}^{r1} = \frac{1 + \frac{T_{r1}}{T_s}}{1 + \frac{T_{r1}}{T_{r2}}} > 1$

$R_{y,o}^x > 0$ and $R_{z,o}^y < 1$, then Eq. (4) yields $1 > R_{z,o}^x > R_{z,o}^y$. Since both $R_{y,o}^x$ and $R_{z,o}^y$ can assume three possible ratio ranges, D , OD and N , nine speed ratio relations can be derived from Eq. (4) as shown in Table 7.

4.2 CLUTCH-TO-CLUTCH SHIFT. A clutch-to-clutch shift occurs when one rotating clutch is turned on while another rotating clutch is simultaneously turned off between two successive speed ratios. That is the input link is switched from one of the coaxial links to another while the fixed and output links remain unchanged. Hence, a clutch-to-clutch shift is feasible when there is one common fixed link between two speed ratios.

Let $R_{z,o}^x$ and $R_{z,o}^y$ denote two such speed ratios. Dividing $1 - R_{z,o}^x$ by $1 - R_{z,o}^y$ and after simplification, we obtain

$$\frac{1 - R_{z,o}^x}{1 - R_{z,o}^y} = 1 - R_{x,o}^y \quad (5)$$

Hence, if the ranges of $R_{y,o}^x$ and $R_{z,o}^y$ are known, the speed ratio relation between $R_{z,o}^x$ and $R_{z,o}^y$ can be derived from Eq. (5). Again, nine speed ratio relations can be derived from Eq. (5) as shown in Table 8.

5 ARRANGEMENT OF CLUTCHING SEQUENCES

We now describe a step-by-step procedure for arranging feasible clutching sequences of an *EGM*.

STEP 1. An *EGM* is decomposed into several *FGEs* [22]. Then, the operation modes and their ratio ranges are identified from Tables 3 through 6.

STEP 2. All possible speed ratios of an *EGM* are expressed in terms of its *FGEs* using the method developed by Hsieh and Tsai [11]. Then, Table 2 is applied to identify the ranges of some of the speed ratios. We note that some speed ratios cannot be identified in this step due to the fact that gear sizes are not specified.

STEP 3. In this step, two speed ratios sharing one

Table 7: Speed Ratio Relations with One Common Input Link

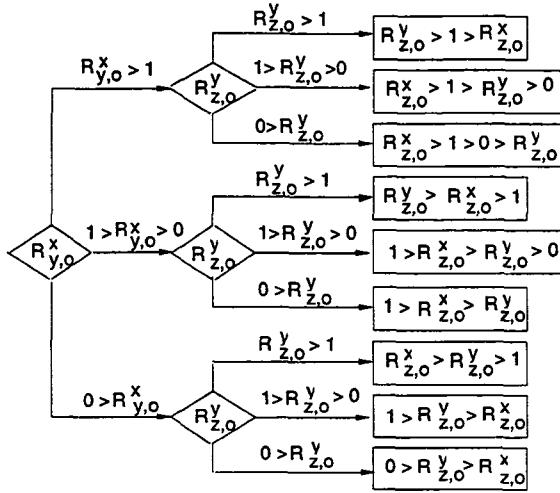
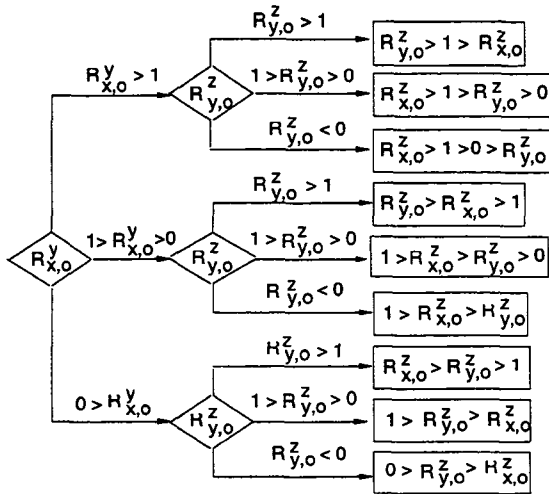


Table 8: Speed Ratio Relations with One Common Fixed Link



common input link are compared and arranged in a descending order. These two speed ratios are the potential candidates for achieving a band-to-band clutching condition. In addition to a predetermined output link, o , we choose three coaxial links, (x, y, z) , from an EGM to construct Table 7. For an EGM with m coaxial links, there are $(m-1)(m-2)(m-3)/6$ possible sets of three coaxial links which can be classified into four groups according to the number of known speed ratio ranges obtained from Step 2.

Group 1: All three speed ratio ranges associated with a set of three coaxial links are known. Let one of the three coaxial links be the common input link and apply Table 7 to arrange their speed ratios in a descending order. By taking one of the three coaxial links as the common input link at a time, three speed ratio relations can be derived.

Group 2: Two of the three speed ratio ranges associated with a set of three coaxial links are known. Let the three coaxial links to assume proper positions of (x, y, z) shown

in Table 7 such that the ranges of $R^x_{y,o}$ and $R^y_{z,o}$ are known. This way, the range of $R^x_{z,o}$ and the speed ratio relation between $R^y_{z,o}$ and $R^x_{z,o}$ can be determined from Table 7. We perform this operation as many times as possible until all possible arrangements of (x, y, z) are exhausted. Note that, after this operation, other sets of three coaxial links containing the newly determined speed ratio, $R^x_{z,o}$, may be re-classified as group 1 members.

Group 3: One of the three speed ratio ranges associated with a set of three coaxial links is known. Let the three coaxial links to assume proper positions of (x, y, z) such that $R^x_{y,o}$ becomes the only known speed ratio. Then, we let $R^y_{z,o}$ to assume three possible ranges, D , OD , and N , and derive the speed ratio relation between $R^y_{z,o}$ and $R^x_{z,o}$ by applying Table 7. Again, after this operation, other sets of three coaxial links containing the newly determined speed ratios, $R^y_{z,o}$ and $R^x_{z,o}$, may be re-classified as group 1 or group 2 members.

Group 4: None of the speed ratio ranges associated with a set of three coaxial links are known. For this case, we derive the speed ratio relation by using two assumed speed ratio ranges, $R^x_{y,o}$ and $R^y_{z,o}$.

Note that, several sets of three coaxial links may depend on the same assumed speed ratio ranges. We further classify such dependent sets and their speed ratio relations into *families*. Thus, an EGM may have several families of speed ratio relations.

STEP 4. Similar to Step 3, two speed ratios sharing one common fixed link are arranged in a descending order by applying Table 8. These two speed ratios are potential candidates for achieving a clutch-to-clutch clutching condition.

STEP 5. In this step, we further classify the speed ratio ranges into three kinds: D , OD and N . A clutching sequence usually includes a *direct drive* between the last reduction and the first overdrive. Thus, the reductions and the overdrives are classified into two different kinds. The speed ratios of the same family and same kind are then arranged in a descending order. To help visualize the speed ratio relations, we sketch the speed ratio ranges in a flow chart wherein two related speed ratios are connected by an arrow pointing from a higher speed ratio to a lower one. Then, we label the arrows with a B or C to denote a *band-to-band* or *clutch-to-clutch* shift. Such a sketch can also help us in realizing the maximum number of feasible reductions and overdrives in a clutching sequence.

STEP 6. A direct drive is obtained by simultaneously clutching two coaxial links of an EGM to the input power source. In order to achieve a single-shift transition, three rules are proposed:

Rule 1: If the input clutches used for the last reduction and the first overdrive are different, we apply these two input clutches for the direct drive.

Rule 2: If the input clutches used for the last reduction and the first overdrive are the same, then apply this input clutch and another clutch used in the other speed ratio for the direct drive.

Rule 3: If there is only one input clutch used for all speed ratios, then add an additional input clutch to the

Table 9: Twelve Possible Speed Ratios Derived From the Mechanism Shown in Fig. 1

Range	Overall speed ratio
D	$R_{1,3}^4, R_{4,3}^1, R_{4,3}^5, R_{5,3}^4$
OD	$R_{2,3}^1, R_{5,3}^1$
P	$R_{2,3}^4$
N	$R_{1,3}^5, R_{1,3}^2$
Unknown	$R_{4,3}^2, R_{2,3}^5, R_{5,3}^2$

mechanism.

STEP 7. Finally, we add a reverse drive to the clutching sequence. In order to reduce the number of rotating and band clutches, we apply two of the clutches designed for the forward drives for the reverse drive.

6 EXAMPLE

The mechanism shown in Fig. 1 is composed of a Simpson gear train and a simple planetary gear train. Assuming that the sizes of the sun gears are in the descending order of gear 1 > gear 1' > gear 4, and the sizes of the ring gears are in the descending order of gear 3 > gear 4 > gear 5. The procedure for deriving possible clutching sequences is as follows:

STEP 1. The three *FGEs* are shown in Fig. 2. Since all three *FGEs* belong to the operation mode shown in Table 3(a), we have $R_{3,1}^2 < 0$, $R_{4,1'}^3 < 0$, and $R_{5,4}^3 < 0$. All the other speed ratios of the *FGEs* due to kinematic inversion can be found from Table 2.

STEP 2. Since there are five coaxial links and link 3 has already been assigned as the output link, a total of twelve clutching conditions and, therefore, twelve overall speed ratios are possible. Each of these speed ratios can be expressed in terms of the above three *FGEs* using the methodology developed by Hsieh and Tsai [11]. After some algebra, we obtain twelve speed ratios grouped according to their ratio ranges as shown in Table 9.

STEP 3. Selecting three out of the four coaxial links at one time, yields four sets of three coaxial links which can be divided into three groups. The first group includes one set of three coaxial links (1, 4, 5), the second group includes two sets of three coaxial links (1, 2, 4) and (1, 2, 5), and the third group includes one set of three coaxial links (2, 4, 5).

For the coaxial links (1, 4, 5), we use the fact that $R_{4,3}^1 > 1$ and $R_{5,3}^4 > 1$ from Table 9 to begin our evaluation. By assigning $x = 1$, $y = 4$, and $z = 5$ in Table 7, we obtain $R_{5,3}^4 > 1 > R_{1,3}^5$. Assigning $x = 5$, $y = 4$, and $z = 1$ in Table 7, we obtain $R_{1,3}^5 > 1 > R_{4,3}^1$. And assigning $x = 5$, $y = 1$, and $z = 4$ in Table 7, we obtain $R_{4,3}^1 > R_{4,3}^5 > 1$.

For the coaxial links (1, 2, 5), we obtain $R_{1,3}^2 < 0$ and $1 > R_{5,3}^1 > 0$ from Table 9. By assigning $x = 2$, $y = 1$, and $z = 5$ in Table 7, we obtain $1 > R_{5,3}^1 > R_{2,3}^5$. By assigning $x = 5$, $y = 1$, and $z = 2$ in Table 7, we obtain $1 > R_{2,3}^5 > R_{5,3}^1$. Note that from the above two operations the range of $R_{2,3}^5$ is identified as $R_{2,3}^5 < 1$. Two possible subcases exist: (1) $1 > R_{2,3}^5 > 0$ and (2) $0 > R_{2,3}^5$. We let $x = 5$, $y = 2$, $z = 1$ in Table 7 and evaluate each subcase

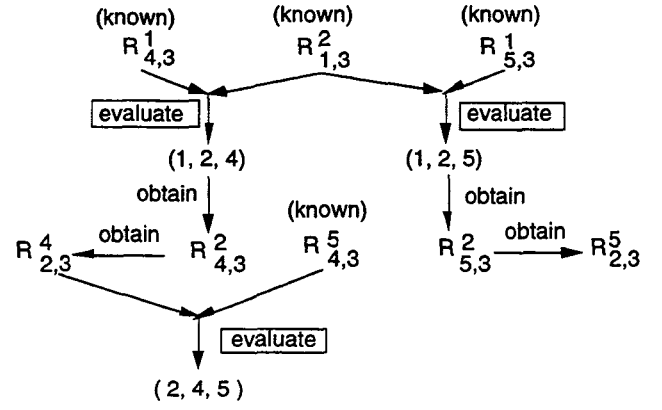


Figure 3: Speed Ratio Evaluation For the Mechanism Shown in Fig. 1

separately. If $1 > R_{2,3}^5 > 0$, then $0 > R_{1,3}^5 > R_{2,3}^5$; and if $0 > R_{2,3}^5$, then $0 > R_{1,3}^5 > R_{5,3}^1$. After this step, the ranges of $R_{2,3}^5$ and $R_{5,3}^1$ become known.

Similarly, the ranges of $R_{4,3}^2$ and $R_{2,3}^4$ are obtained by performing the second-group evaluation for the coaxial links (1, 2, 4).

For each subcase, we obtain the ranges of $R_{4,3}^2$, $R_{2,3}^4$, $R_{5,3}^2$, and $R_{2,3}^5$ which enable us to perform the first-group evaluation for the set of three coaxial links (2, 4, 5). The sequence of evaluation are schematically depicted in Fig. 3.

STEP 4. In this step, we compare two speed ratios with a common fixed link. The procedure is similar to that of Step 3. For example, the two speed ratios $R_{1,3}^4$ and $R_{2,3}^4$ can be compared by applying Table 8 to the set of three coaxial links (1, 2, 4).

STEP 5. After completing the speed ratio evaluations, we obtain two families of speed ratio ranges. In each family, there are six drives (D), three overdrives (OD), and three reverses (N) as shown in Tables 10 and 11. We note that there are two sets of three reductions in each family.

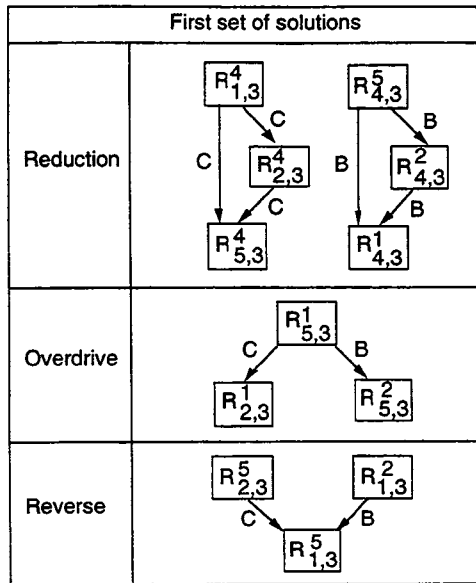
STEP 6. In this step, we add a direct-drive between the last reduction and the overdrive. For example, the input clutches C_1 and C_2 shown in Table 1 are applied for the direct drive based on Rule 3. Hence, with one overdrive, we obtain four feasible four-speed clutching sequences as shown in Table 12. If two overdrives are permitted, eight five-speed clutching sequences are feasible.

STEP 7. Finally, a reverse drive is added to each clutching sequence. Table 1 shows one feasible clutching sequence with rotating clutches attached to links 1 and 4, and band clutches attached to links 1, 2, and 5. This clutching sequence has been applied in several four-speed transmissions.

7 RESULTS

A computer program for the enumeration of clutching sequences has been written in MATHEMATICA language [27]. The algorithm obviates the necessity of inputting the exact gear dimensions of an *EGM*. The designer only needs to specify the vertex-to-vertex adjacent matrix of an *EGM*, the number and type of gears on each link, and the information containing the approximate gear sizes are

Table 10: Speed Ratio Flow Chart Derived From the Mechanism Shown in Fig. 1 - Family 1



ranged in a descending order. The program starts with the identification of the various operation modes of an *EGM* and arriving at all feasible clutching sequences. We have tested the program on various gear trains. As a result, we obtain two three-speed and two four-speed clutching sequences for each of the Simpson, Ravigneaux, and Type-6206 gear sets [1] as shown in Figs. 4, 5, and 6.

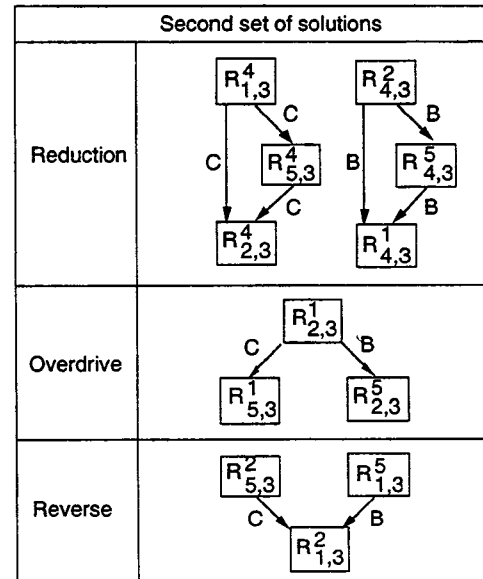
The clutching sequence shown in Figs. 4(b) and 5(b) have been used in most three-speed automatic transmissions (See [1] for examples). The clutching sequence shown in Fig. 6(b) has been applied in the HYDRA-MATIC 3L80 transmission. The clutching sequence shown in Fig. 6(d) has been used in HYDRA-MATIC 4T60 and Ford Axod. The other clutching sequences shown appear to be new.

8 CONCLUSION

In this study, we have concentrated on three issues related to the enumeration of clutching sequences associated with epicyclic gear mechanisms from the kinematic point of view.

First, a procedure for estimating the overall speed ratio of an *EGM*, without specifying the exact gear dimensions, is outlined. Then, an algorithm for comparing various possible speed ratios of an *EGM* is described. Finally, a methodology for systematically enumerating all possible clutching sequences of an *EGM* is established. The methodology has been demonstrated by a transmission gear set making up of three simple planetary gear trains. In addition, a computer program has been written in MATHEMATICA [27] and successfully tested on various transmission gear trains including the Simpson, Ravigneaux, and Type-6206 gear sets. It is shown that all possible clutching sequences of an *EGM* can be systematically enumerated. It is hoped that this methodology will provide transmission designers an efficient tool for enumer-

Table 11: Speed Ratio Flow Chart Derived From the Mechanism Shown in Fig. 1 - Family 2



ating feasible clutching sequences of an *EGM*.

In this paper, the physical layout of a transmission mechanism has not been studied. It is possible that some of the clutching sequences enumerated may lead to infeasible mechanical layout. This is a subject of future study.

9 NOMENCLATURE

D	Drive, $R_{x,y}^z > 1$
EGM	Epicyclic gear mechanism
FGE	Fundamental geared entity
N	Reverse, $R_{x,y}^z < 0$
OD	Overdrive, $1 > R_{x,y}^z > 0$
P	Positive speed ratio, $R_{x,y}^z > 0$
$N_{p,x}$	Gear ratio defined by a planet gear p and a sun or a ring gear x . $N_{p,x} = \pm T_p/T_x$, where T_p and T_x denote the number of teeth on a planet gear and a sun or ring gear, respectively, and the positive or negative sign depends on whether x is a ring or sun gear.
$R_{x,y}^z$	Speed ratio between an input link x and an output link y with reference to a fixed link z , $R_{x,y}^z = (\omega_x - \omega_z)/(\omega_y - \omega_z)$.
c	Carrier
r	Ring gear
s	Sun gear
ω_i	Angular velocity of link i

10 ACKNOWLEDGMENT

This work was supported in part by the U.S. Department of Energy under Grant No. DEF05-88 ER 13977. Such support does not constitute an endorsement by the supporting agency of the views expressed in the paper.

Table 12: Four Four-Speed Clutching Sequences Derived From the Mechanism Shown in Fig. 1

First set of solutions

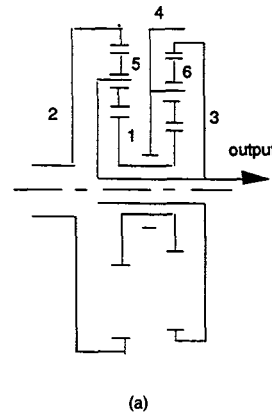
Gear	Activated clutches				
	C ₁	C ₂	B ₁	B ₂	B ₃
First	X ₄		X ₅		
Second	X ₄			X ₂	
Third	X ₄				X ₁
Fourth	X ₄	X ₁			
Reverse		X ₁	X ₅		

Gear	Activated clutches				
	C ₁	C ₂	C ₃	B ₁	B ₂
First	X ₁			X ₄	
Second		X ₂		X ₄	
Third			X ₅	X ₄	
Fourth		X ₂	X ₅		
Reverse	X ₁				X ₅

Second set of solutions

Gear	Activated clutches				
	C ₁	C ₂	B ₁	B ₂	B ₃
First	X ₄		X ₂		
Second	X ₄			X ₅	
Third	X ₄				X ₁
Fourth	X ₄	X ₁			
Reverse		X ₁		X ₅	

Gear	Activated clutches				
	C ₁	C ₂	C ₃	B ₁	B ₂
First	X ₁			X ₄	
Second		X ₅		X ₄	
Third			X ₂	X ₄	
Fourth		X ₅	X ₂		
Reverse	X ₁				X ₅



Activated clutches				
Gear	C ₁	C ₂	B ₁	B ₂
First	X ₂			X ₄
Second	X ₂			X ₁
Third	X ₂	X ₁		
Reverse		X ₁	X ₄	

(b)

Activated clutches				
Gear	C ₁	C ₂	B ₁	B ₂
First	X ₁		X ₂	
Second		X ₄	X ₂	
Third	X ₁	X ₄		
Reverse	X ₁			X ₄

(c)

Activated clutches					
Gear	C ₁	C ₂	B ₁	B ₂	B ₃
First	X ₁		X ₂		
Second		X ₄	X ₂		
Third	X ₁	X ₄			
Fourth		X ₄		X ₁	
Reverse	X ₁				X ₄

(d)

Activated clutches					
Gear	C ₁	C ₂	C ₃	B ₁	B ₂
First	X ₂			X ₄	
Second	X ₂				X ₁
Third	X ₂	X ₄			
Fourth		X ₄			X ₁
Reverse			X ₁	X ₄	

(e)

11 REFERENCES

1. Tsai, L.W., Maki, E. R., Liu, T., and Kapil, N. G., "The Categorization of Planetary Gear Trains For Automatic Transmissions According to Kinematic Topology," SAE paper No. 885062, *SAE XXII FISITA '88, Automotive Systems Technology: The Future, P-211*, Vol. 1, pp. 1.513-1.521, 1988.
2. Levai, Z., "Theory of Epicyclic Gears and Epicyclic Change-Speed Gears", Doctoral Dissertation, Budapest, 1964.
3. Gackstetter, G., "Leistungsverzweigung bei der stufenlosen Drehzahlregelung mit vierwelligen Planetengetrieben," VDI-Z, Vol. 108, No.6, pp. 210-214, 1966.
4. Polder, J.W., "A Network Theory for Variable Epicyclic Gear Trains," Ph.D. Dissertation, University of Technology, Eindhoven, Netherland, 1969.
5. Freudenstein, F., and Yang, A. T., "Kinematics and Statics of Coupled Epicyclic Spur Gear Trains," *Journal of Mechanism and Machine Theory*, Vol. 7, pp. 263-375, 1972.
6. Tsai, L.W., "An Algorithm for the Kinematic Analysis of Epicyclic Gear Trains," *Proc. Sixth Applied Mechanisms Conference*, Kansas City, 1985.
7. Belfiore, N. P., and Pennestri, E., "Kinematic and Static Force Analysis of Epicyclic Gear Trains," *Proceedings 1st National Applied Mechanisms and Robotics*, Cincinnati, OH, Vol. 1, Paper No. AMR-6B-1, 1989.
8. Hedman, A., "Mechanical Transmission Systems: A General Computer Based Method of Analysis," Ph.D. Dissertation, Div. of Machine Elements, Chalmers University of Technology, Goteborg, Sweden, 1989.
9. Hedman, A., "Computer Aided Analysis of General Mechanical Transmission Systems," *Proc. Second Int'l Conf. on New Developments in Powertrain and Chassis Engineering*, Strassburg, France, pp. 193-197, 1989.
10. Hedman, A., "Transmission Analysis - Automatic Derivation of Relationships," *ASME Journal of Mechanical Design*, Vol. 115, No. 4, pp. 1031-1037, 1993.
11. Hsieh, H.I., and Tsai, L.W., "Kinematic Analysis of Epicyclic-Type Transmission Mechanisms Using the Concept of Fundamental Geared Entities," *Proc. of the ASME 1995 Design Eng. Tech. Conferences, Advances in Design Automation*, Vol. 1, pp. 545-552, Boston, Mass, 1995.
12. Saggere, L., and Olson, D. G., "A Simplified Approach for Force and Power-Flow Analysis of Compound Epicyclic Spur-Gear Trains," *Proc. ASME Advances in Design Automation*, DE-Vol. 44-2, pp. 83-89, 1992.
13. Pennestri, E., and Freudenstein, F., "A Systematic Approach to Power-Flow and Static Force Analysis in Epicyclic Spur-Gear Trains," *ASME Journal of Mechanical Design*, Vol. 115, No. 3, pp. 639-644, 1993.
14. Pennestri, E., Sinatra, R., and Belfiore, N. P., "A Catalog of Automotive Transmissions with Kinematic and Power-Flow Analysis," *Proc. National Applied Mechanisms and Robotics*, Cincinnati, OH, No. AMR-93-057, pp. 1-8, 1993.

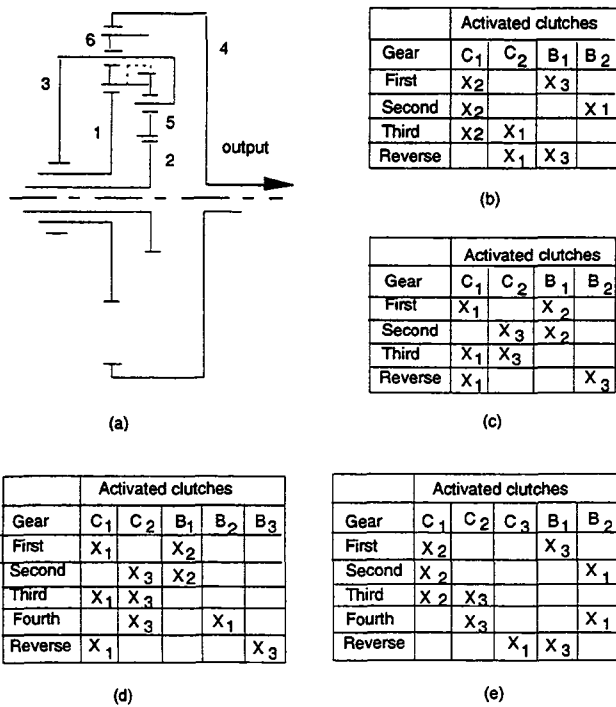


Figure 5: Four Feasible Clutching Sequences Derived From Ravigneaux Gear Set

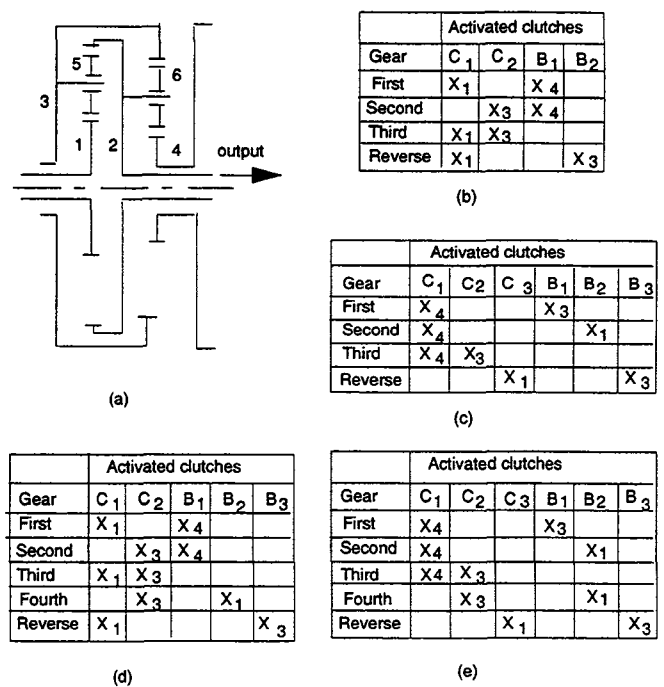


Figure 6: Four Feasible Clutching Sequences Derived From Type 6206 Gear Set

15. Buchsbaum, F., and Freudenstein, F., "Synthesis of Kinematic Structure of Geared Kinematic Chains and Other Mechanisms," *Journal of Mechanisms and Machine Theory*, Vol. 5, pp. 357-392, 1970.
16. Mruthyunjaya, T.S., and Ravisankar, R., "Computerized Synthesis of the Structure of Geared Kinematic Chains," *Journal of Mechanisms and Machine Theory*, Vol. 20, pp. 367-387, 1985.
17. Tsai, L.W., and Lin, C.C., "The Creation of Non-Fractionated Two-Degree-of-Freedom Epicyclic Gear Trains," *ASME J. of Mechanisms, Transmissions, and Automation in Design*, Vol. 111, pp. 524-529, 1989.
18. Hylander, M., "Generation and Optimization of Epicyclic Transmission Designs," VDI Berichte 1007, 1992.
19. Hylander, M., "On Synthesis in Epicyclic Transmission Design," *Machine and Vehicle Design*, Chalmers University of Technology, Goteborg, Sweden, Report No. 1993-02-26, 1993.
20. Mogalapalli, S.N., Magrab, E.B., and Tsai, L.W., "A CAD System for the Optimization of Gear Ratios for Automotive Automatic Transmissions," *SAE Int'l. Congress and Exposition*, SAE paper No. 930675, Automotive Transmissions and Drivelines, SP-965, pp. 111-118, 1993.
21. Chatterjee, G., and Tsai, L.W., "Enumeration of Epicyclic-Type Automatic Transmission Gear Trains," *SAE International Congress and Exposition*, Paper No. 941012, Transmission and Driveline Developments, SP- 1032, pp. 153-164, 1994.
22. Chatterjee, G., and Tsai, L.W., "Computer-Aided Sketching of Epicyclic-Type Automatic Transmission Gear Trains," *Proc. of the ASME 1994 Design Technical Conferences*, DE-Vol. 71, Machine Elements and Machine Dynamics, pp. 275-282, 1994.
23. Nadel, B.A., and Lin, J., "Automobile Transmission Design as a Constraint Satisfaction Problem: First Results," *Proc. 7th IEEE Conf. on Artificial Intelligence Applications*, pp. 248-256, 1991.
24. Nadel, B.A., and Lin, J., "Automobile Transmission Design as a Constraint Satisfaction Problem: Modeling the Kinematic Level," *Artificial Intelligence for Engineering Design, Analysis and Manufacturing*, Vol. 5, No. 3, pp. 137-171, 1991.
25. Nadel, B.A., Wu, X., and Kagan, D., "Multiple Abstraction Levels in Automobile Transmission Design: Constraint Satisfaction Formulation and Implementation," *Int'l. Journal of Expert Systems*, Vol. 6, No. 4, pp. 489- 559, 1993.
26. Tsai, L.W., "The Kinematics of Spatial Robotic Bevel-Gear Trains," *IEEE Journal of Robotics and Automation*, Vol. 4, No. 2, pp. 150-155, 1988.
27. Wolfram, S., "Mathematica: A System For Doing Mathematics By Computer," Addison-Wesley, New York, NY, 1991.

